

A numerical method for solving distributed order time fractional COVID-19 virus model based on Legendre wavelets optimization approach

M. Khasteh, A.H. Refahi Sheikhani*, F. Shariffar

Received: 16 August 2023; Accepted: 9 January 2024

Abstract In this paper, we introduced a distributed order time fractional Coronavirus-19 disease transmission involving Caputo-Prabhakar fractional derivative of α order in time t . The coronavirus 19 disease model has 8 inger dents leading to system of 8 nonlinear ordinary differential equations in this sense. To solve these types of equations, we proposed a numerical method based on the upon Legendre wavelets optimization approximations. In the first stage, by applying the Legendre wavelets optimization functions and Laplace transform an exact formula for the Prabhakar fractional integral operator is derived. Then, we apply this exact formula and the properties of Legendre wavelets optimization functions to change the given equation into a system of algebraic equations. We calculated the approximation optimal solutions of our system applying the Newton's iterative method. The optimal approximate solutions obtained by using the proposed method are considered as the best solutions for the proposed equation. Error analysis is examined to verify the practical efficiency of the proposed method. In the end, for the efficiency and performance of the proposed method, the numerical results are shown in the figure.

Keyword: COVID-19 Virus, Distributed-Order, Legendre Wavelets Optimization Approach, Caputo-Prabhakar Derivative, Error Analysis.

1 Introduction

In this Section, we consider the following distributed order time fractional Coronavirus-19 disease (COVID-19) model:

$$\begin{aligned}\mathbb{D}^{\omega(\alpha)}S(t) &= -S(t)(\alpha_1I(t) + \alpha_2D(t) + \alpha_3A(t) + \alpha_4R(t)), \\ \mathbb{D}^{\omega(\alpha)}I(t) &= S(t)(\alpha_1I(t) + \alpha_2D(t) + \alpha_3A(t) + \alpha_4R(t)) - (\epsilon_1 + \zeta_1 + \lambda_1)I(t), \\ \mathbb{D}^{\omega(\alpha)}D(t) &= \epsilon_1I(t) - (\eta_1 + \rho_1)D(t), \\ \mathbb{D}^{\omega(\alpha)}A(t) &= \zeta_1I(t) - (\theta_1 + \mu_1 + \kappa_1)A(t), \\ \mathbb{D}^{\omega(\alpha)}R(t) &= \eta_1D(t) + \theta_1A(t) - (\nu_1 + \xi_1)R(t),\end{aligned}\tag{1}$$

* Corresponding Author. (✉)

E-mail: ah_refahi@yahoo.com (A.H. Refahi Sheikhani)

M. Khasteh

Department of Applied Mathematics, Faculty of Mathematical Sciences, Lahijan Branch, Islamic Azad University, Lahijan, Iran

A.H. Refahi Sheikhani

Department of Applied Mathematics, Faculty of Mathematical Sciences, Lahijan Branch, Islamic Azad University, Lahijan, Iran

F. Shariffar

Department of Applied Mathematics, Fouman and Shaft Branch, Islamic Azad University, Fouman, Iran

$$\begin{aligned}\mathbb{D}^{\omega(\alpha)}T(t) &= \mu_1 A(t) + \nu_1 R(t) - (\sigma_1 + \tau_1)T(t), \\ \mathbb{D}^{\omega(\alpha)}H(t) &= \lambda_1 I(t) + \rho_1 D(t) + \kappa_1 A(t) + \xi_1 R(t) + \sigma_1 T(t), \\ \mathbb{D}^{\omega(\alpha)}E(t) &= \tau_1 T(t),\end{aligned}$$

subject to the initial conditions:

$$S(0) = S_0, I(0) = I_0, D(0) = D_0, A(0) = A_0, R(0) = R_0, T(0) = T_0, H(0) = H_0, E(0) = E_0, \quad (2)$$

in which all parameters are positive and their physical interpretation are studied in [1]. In Equation (1), the function $S(t)$ is the class of susceptible, the function $D(t)$ is the class of asymptomatic infected, the function $I(t)$ is the class of infected asymptomatic infected undetected, detected, the function $A(t)$ is ailing symptomatic infected, undetected, the function $R(t)$ is recognized symptomatic infected, detected, the function $T(t)$ is the class of acutely symptomatic infected detected, the function $H(t)$ is the healed class and the function $E(t)$ is the death class. Also, and $\mathbb{D}^{\omega(\alpha)}$ shows the distributed order Caputo-Prabhakar fractional operator of α order in time t such that $\alpha \in (0,1]$.

The COVID-19 are a large collection of viruses which have a specified corona or 'crown' of sugary-proteins and because of their form, they were called COVID-19 in 1960. Due to the world health organization (WHO), COVID-19 is spreaded via people who have been infected with the corona virus. The virus may quickly transmit via small drops from the mouth compilation or nose of anybody infected via this virus to cough or sneeze. The small drops then land on surfaces or objects which are touched and the healthy person regulates their nose, mouth or eyes. For the first time in the Wuhan city the COVID-19 was appeared that this virus has not been previously known in humans. Bats or snakes have been skepticed as a potential source for the prevalence, though other experts currently consider this unlikely. Cough, fever, breathing difficulties and shortness of breath are the initial signs of this infection. In the next stages, the infection may reason pneumonia, kidney failure, even death and severe acute respiratory syndrome.

Differential equations with distributed order fractional derivatives and obtaining their numerical solutions using the analytical and numerical methods are a useful tool to describe important applications in the different fields of physics [2, 3], chemistry [4], mathematics [5] and engineering [6]. For the first time in 1960s by Caputo's is studied the distributed-order differential equation [7] to expand the stress-strain equation of inelastic media. Later in [8], the multi-term viscoelastic equation of fractional order as a model of distributed-order equation is developed. the differential equation of distributed-order is considered as a extension of the differential equation of multi-term fractional order. Recently, the numerical schemes obtaining the numerical solutions for a class of distributed order fractional differential equation with fractional derivative have been studied, for example, Fei et al. [9] studied a numerical method based on the Galerkin-Legendre spectral method to numerically solve a two-dimensional time fractional fourth-order partial differential equation of distributed-order. Zaky et al. [10] studied a numerical method based on the Legendre spectral-collocation method to numerically solve a distributed-order fractional initial value problems. Zhang et al. [11] studied a numerical method based on the Crank-Nicolson ADI Galerkin-Legendre spectral method to numerically solve a two-dimensional Riesz space distributed-order advection-diffusion equation. The nonlinear fractional differential equations of distributed-order are solved by using Legendre-Gauss collocation method by Xu et al. [12]. Dehghan et al. [13] studied a numerical method for solving fractional damped diffusion-wave equation of distributed-order by using spectral element method. Guo et al. [14] studied a solution for the two-dimensional distributed-order time-space fractional reaction-diffusion equation by using Legendre spectral element method. Morgado et al. [15] studied a solution

for the distributed order time-fractional diffusion equation by using Chebyshev collocation method. Mashayekhi et al. [16] studied the synthetic of block-pulse functions and Bernoulli polynomials, Gorenflo et al. [17] studied the Fourier and Laplace transforms for solving the one-dimensional distributed order diffusion-wave equation, Li et al. [18] proposed a classical numerical quadrature method, Aminikhah et al. [19] used a combined method based on the Laplace transform and new homotopy perturbation method To solve a particular class of the distributed order fractional Riccati equation, Mashoo et al. [20] studied the stability of two classes of distributed-order Hilfer-Prabhakar differential equations, Mashoo et al. [21] proposed the stability of distributed order differential equations form of Hilfer-Prabhakar, Aminikhah et al. [22] proposed two numerical methods to solve the distributed-order fractional Bagley-Torvik equation by the fractional differential transform and Grunwald-Letnikov method, Ye et al. [23] applied a compact difference method, Mashoof et al. [24] studied an operational matrix for solving the fractional differential equations of distributed order, Yuttanan et al. [25] studied a numerical method based on the upon Legendre wavelets polynomials for solving linear and nonlinear distributed fractional differential equations, the existence and uniqueness for differential equations of distributed order proposed by Ford et al. [26], the uniqueness of solutions for time-fractional diffusion equations of distributed order on bounded domains proposed by Luchko [27], Bhrawy et al. [28] proposed a numerical method based on the Jacobi-Gauss-Lobatto collocation method to solve Schrödinger equations of distributed order and Kharazmi et al. [29] studied a solution for the fractional partial differential equations of distributed order by using pseudo-spectral method.

The main aim of this paper is to study an efficient numerical method to numerically solve Equations (1) and (2). This efficient numerical method is based upon Legendre wavelets optimization approach. For the first time, we derive an exact formula for the Prabhakar fractional integral operator in terms of Legendre wavelets optimization functions. Then, by using this exact formula for the Prabhakar fractional integral operator, we transform the solution of the distributed order time fractional Coronavirus-19 disease model to the solution of algebraic equations.

The outline of this paper is organized as follows. In Section 2, we briefly introduce the mathematical preliminaries and some necessary definitions which are required for our problem. Also, in this Section, we express the wavelets and Legendre wavelets optimization functions. In Section 3, we express the approximation function and also, we describe the Riemann-Liouville fractional integral operator for Legendre wavelets optimization functions. In Section 4, we derive a numerical method to numerically solve Equations (1) and (2). In Section 5, the error bound is studied. In Section 6, some examples are demonstrated to show the reliability and validity of the proposed method. In the end, in Section 7, the main and important conclusions of the proposed method are highlighted.

2 Preliminaries

In this Section, we study the basic, important definitions and some essential lemmas of fractional calculus which will applied for later. Moreover, we display important properties of the wavelets and Legendre wavelets optimization functions.

Definition 1 [30-33] Let $\alpha \in (n-1, n]$, $n \in \mathbb{N}$ and $u \in L^1[0, b]$ such that $-\infty \leq 0 < x < b \leq \infty$. Then, for a function u , the Riemann-Liouville fractional integral of order α and Riemann-Liouville fractional derivative of order α are given respectively by

$${}_0I_x^\alpha u(x) = \frac{1}{\Gamma(\alpha)} \int_0^x (x-\tau)^{\alpha-1} u(\tau) d\tau, \quad (3)$$

$${}_0D_x^\alpha u(x) = \frac{1}{\Gamma(n-\alpha)} \frac{d^n}{dx^n} \int_0^x (x-\tau)^{n-1-\alpha} u(\tau) d\tau. \quad (4)$$

Definition 2 For $\alpha \in (0,1]$ and $u \in C(0,b)$. Then, the Caputo fractional derivative of order α is given by

$${}_0^C D_x^\alpha f(x) = {}_0 I_x^{1-\alpha} \frac{d}{dx} u(x) = \frac{1}{\Gamma(1-\alpha)} \int_0^x (x-\tau)^{-\alpha} \frac{d}{d\tau} u(\tau) d\tau. \quad (5)$$

In the recent years, one of the fractional operators that has attracted the attention of many authors is Prabhakar fractional operator. This fractional operator is as generalization of derivatives of both Riemann–Liouville and Caputo types. Indeed, this type of derivative is similar to the Riemann–Liouville derivative with a more general integral operator with the kernel

$$e(\gamma, \rho, \alpha, \omega) = x^{\alpha-1} E_{\rho, \alpha}^\gamma, \quad \rho, \alpha, \omega, \gamma \in \mathbb{C},$$

in which $E_{\rho, \alpha}^\gamma$ is the Prabhakar function and studied by Prabhakar in 1971 [34],

$$E_{\rho, \alpha}^\gamma(x) = \sum_{k=0}^{\infty} \frac{\Gamma(\gamma+k)}{\Gamma(\gamma)\Gamma(\rho k+\alpha)} \frac{x^k}{k!}, \quad \operatorname{Re}(\rho), \operatorname{Re}(\alpha) > 0. \quad (6)$$

In case $\gamma = 0$ we have

$$E_{\rho, \alpha}^0(x) = \frac{1}{\Gamma(\alpha)}.$$

Moreover, in case $\gamma = 1$, we find the widely known function as two-parameter Mittag–Leffler, i.e.

$$E_{\rho, \alpha}^1(x) = E_{\rho, \alpha}(x) = \sum_{k=0}^{\infty} \frac{1}{\Gamma(\rho k+\alpha)} x^k,$$

by putting $\alpha = \gamma = 1$, Eq. (6) converts to the classical Mittag–Leffler function, i.e.

$$E_{\rho, 1}^1(x) = E_\rho(x) = \sum_{k=0}^{\infty} \frac{1}{\Gamma(\rho k+1)} x^k.$$

Definition 3 Suppose that $n-1 < \operatorname{Re}(\alpha) < n, n \in \mathbb{N}$ and $u \in L^1[0, b], -\infty \leq a < x < b \leq \infty$. Then the Prabhakar fractional integral of order α with $\rho, \alpha, \omega, \gamma \in \mathbb{C}$ is defined by

$$E_{\rho, \alpha, \omega, 0}^\gamma u(x) = \int_a^x (x-\tau)^{\alpha-1} E_{\rho, \alpha}^\gamma(\omega(x-\tau)^\rho) u(\tau) d\tau, \quad \operatorname{Re}(\rho), \operatorname{Re}(\alpha) > 0, \quad (7)$$

in which $E_{\rho, \alpha}^\gamma$ is defined in (6).

Definition 4 For $u \in L^1[0, b]$ the Prabhakar fractional derivative of order α with $\rho, \alpha, \omega, \gamma \in \mathbb{C}$ is defined by

$${}_0^P D_{\rho, \alpha, \omega}^\gamma u(x) = \frac{d^n}{dx^n} E_{\rho, n-\alpha, \omega, a}^{-\gamma} u(x), \quad x > a. \quad (8)$$

Definition 5 The Caputo–Prabhakar derivative of order α with $\rho, \alpha, \omega, \gamma \in \mathbb{C}$ is defined by

$${}_0^C D_{\rho, \alpha, \omega}^\gamma u(x) = E_{\rho, n-\alpha, \omega, a}^{-\gamma} \frac{d^n}{dx^n} u(x), \quad (9)$$

It has the following property

$$\mathbb{E}_{\rho, \alpha, \omega, a}^{\gamma} {}_{0}^{CP} \mathbb{D}_{\rho, \alpha, \omega}^{\gamma} u(x) = u(x) - u(0), \quad x > 0. \quad (10)$$

Definition 6 The distributed order derivative of order $\omega(\alpha) > 0$ that $\omega(\alpha) > 0$ is the distribution function of order $0 < \alpha \leq 1$, of function $u(t)$ is given by [35]:

$$\mathbb{D}^{\omega(\alpha)} u(t) = \int_0^1 \omega(\alpha) {}^{CP} \mathbb{D}_{\rho, \alpha, \omega}^{\gamma} u(t) d\alpha, \quad (11)$$

in which ${}^{CP} \mathbb{D}_{\rho, \alpha, \omega}^{\gamma}$ is the Caputo–Prabhakar derivative of u of order $0 < \alpha \leq 1$ with $\rho, \alpha, \omega, \gamma \in \mathbb{C}$, $\omega(\alpha) > 0$ is the weight function and

$$\int_0^1 \omega(\alpha) d\alpha = C, C > 0. \quad (12)$$

Also, the Laplace transform of the Caputo–Prabhakar derivative of order $0 < \alpha \leq 1$ with respect to t is given by:

$$\mathcal{L}\{{}^{CP} \mathbb{D}_{\rho, \alpha, \omega}^{\gamma} u(t); s\} = s^{\alpha} (1 - \omega s^{-\rho})^{\gamma} U(s) - s^{\alpha-1} (1 - \omega s^{-\rho})^{\omega} u(0), \quad (13)$$

in which $U(s)$ is the Laplace transform of u and defined by $U(s) = \int_0^{\infty} e^{-st} u(\tau) d\tau$.

Lemma 1 [34] Let $\rho, \alpha, \omega, \gamma \in \mathbb{C}$ and $\Re(\alpha) > 0, \Re(s) > 0$. Then, we have:

$$\mathcal{L}\{t^{\alpha-1} E_{\rho, \alpha}^{\gamma}(\omega x^{\rho}); s\} = s^{-\alpha} (1 - \omega s^{-\rho})^{-\omega}, |\omega s^{-\rho}| < 1.$$

2.1 Wavelets and Legendre wavelets optimization functions

This Section recall a description and study of the wavelets and Legendre wavelets optimization functions. Wavelets constitute a collection of functions made from translation of a single function and dilation called the mother wavelet. When the dilation parameter a and the translation parameter b vary continuously, we have the following collection of wavelets that these collection of wavelets are continuous, as follows [36]:

$$\Psi_{a,b}(t) = |a|^{-\frac{1}{2}} \Psi\left(\frac{t-b}{a}\right), \quad (14)$$

where $a, b \in \mathbb{R}$ and $a \neq 0$. Limitation of the constants a and b to discrete values such as $a = a_0^{-l}, b = nb_0 a_0^{-l}$ and $l, n \in \mathbb{N}$, where $a_0 > 1, b_0 > 0$ yields the following family of discrete wavelets:

$$\Psi_{l,n}(t) = |a_0|^{\frac{l}{2}} \Psi(a_0^l t - nb_0), \quad (15)$$

where in Equation (15), the function $\Psi_{l,n}(t)$ is the wavelet basis for $L^2(\mathbb{R})$. Let $M, l > 0$. Then, the Legendre wavelets optimization functions $\Psi_{n,m}(t)$ on the interval $[0, t_f]$ for $n = 1, 2, 3, \dots, 2^{l-1}$ and $m = 0, 1, 2, \dots, M-1$ are defined as:

$$\Phi_{n,m}(t) = \begin{cases} 2^{\frac{l}{2}} \sqrt{m + \frac{1}{2}} \mathbb{P}_m\left[\frac{2^l}{t_f} t - 2n + 1\right], & t \in [\frac{2^{n-2}}{2^l} t_f, \frac{2^n}{2^l} t_f), \\ 0, & \text{otherwise,} \end{cases} \quad (16)$$

in which $\mathbb{P}_m(t)$ in Equation (16) are the famous Legendre polynomials of order m . The Legendre polynomials of order m satisfy the following recursive relation:

$$\begin{aligned} \mathbb{P}_0(t) &= 1, \mathbb{P}_1(t) = t, \\ \mathbb{P}_{m+1}(t) &= \frac{2m+1}{m+1} t \mathbb{P}_m(t) - \frac{m}{m+1} \mathbb{P}_{m-1}(t), \end{aligned} \quad (17)$$

and the analytic form of the Legendre polynomials of order m is given as:

$$\mathbb{P}_{m+1}(t) = 2^m \sum_{k=0}^m t^k \binom{m}{k} \binom{m+k-1}{2},$$

where $\binom{m}{k} = \frac{m(m-1)\dots(m-k+1)}{k!}$. Also, the family of Legendre wavelets optimization functions

with respect to the weight function are an orthonormal family.

3 Function approximation

Let $\mathbb{W}_{l,M} \subseteq L^2(0,1)$ be the space spanned by a family of $\Psi_{n,m}(t)$ for $n = 1, 2, 3, \dots, 2^{l-1}$ and $m = 0, 1, 2, \dots, M-1$ that the space $\mathbb{W}_{l,M}$ is defined by:

$$\mathbb{W}_{l,M} = \text{span}\{\Psi_{1,0}(t), \dots, \Psi_{2^{l-1},0}(t), \Psi_{1,1}(t), \dots, \Psi_{2^{l-1},1}(t), \Psi_{1,M-1}(t), \dots, \Psi_{2^{l-1},M-1}(t)\}.$$

Let $f(t) \in L^2(0,1)$ that the function $f(t)$ is an arbitrary element. Then, we have:

$$\forall z \in \mathbb{W}_{l,M}, \|f - g\| \leq \|f - z\|,$$

where g is a unique best approximation of f . Since f has the unique best approximation as g , then, we have:

$$f(t) \simeq g = \sum_{n=1}^{2^{l-1}} \sum_{m=0}^{M-1} d_{n,m} \Psi_{n,m}(t) = D^T \mathbb{B}(t), \quad (18)$$

where $d_{n,m}$ is the Legendre wavelets optimization functions coefficients and

$$D^T = [d_{1,0}(t), \dots, d_{2^{l-1},0}(t), d_{1,1}(t), \dots, d_{2^{l-1},1}(t), d_{1,M-1}(t), \dots, d_{2^{l-1},M-1}(t)],$$

$$\mathbb{B}(t) = [\Psi_{1,0}(t), \dots, \Psi_{2^{l-1},0}(t), \Psi_{1,1}(t), \dots, \Psi_{2^{l-1},1}(t), \Psi_{1,M-1}(t), \dots, \Psi_{2^{l-1},M-1}(t)]. \quad (19)$$

Due to orthonormality property of the set of Legendre wavelets optimization functions, the coefficients $d_{n,m}$ are given in Equation (18) can be computed applying

$$d_{n,m} = \frac{\langle f(t), \Psi_{n,m}(x) \rangle}{\langle \Psi_{n,m}(x), \Psi_{n,m}(x) \rangle} = \langle f(t), \Psi_{n,m}(x) \rangle = \int_0^1 \Psi_{n,m}(x) f(t) dt, \quad (20)$$

where $\langle \cdot, \cdot \rangle$ shows the inner product of the Hilbert space $L^2[0,1]$.

Theorem 2 Let $\Psi_{n,m}(t)$ be the Legendre wavelets optimization functions which is introduced in Equation (16). Then, we have:

$$\mathcal{L}(\Psi_{n,m}; s) = 2^{\frac{l}{2}+m} \sqrt{m + \frac{1}{2}} e^{-\frac{2nt_f s}{2^l}} \times \sum_{k=0}^m \sum_{r=0}^k \frac{k!}{r!} \binom{m}{k} \left(\frac{m+k-1}{2}\right) \left(\frac{2^l}{t_f}\right)^{k-r} (e^{\frac{2s}{2^l}} (-1)^r - 1) \frac{1}{s^{k-r+1}}, \quad (21)$$

where \mathcal{L} represents the Laplace transform.

Proof. The Legendre wavelets optimization polynomials $\Psi_{n,m}(t)$ in Equation (16) can be rewritten in terms of unit step function λ_c as follows:

$$\Psi_{n,m}(t) = 2^{\frac{l}{2}} \sqrt{m + \frac{1}{2}} \lambda_{\frac{2n-2}{2^l} t_f} \mathbb{P}_m \left[\frac{2^l}{t_f} t - 2n + 1 \right] - \lambda_{\frac{2n}{2^l} t_f} 2^{\frac{l}{2}} \sqrt{m + \frac{1}{2}} \mathbb{P}_m \left[\frac{2^l}{t_f} t - 2n + 1 \right], \quad (22)$$

where λ_c is defined by:

$$\lambda_c = \begin{cases} 1, & t \geq c, \\ 0, & t < c. \end{cases}$$

By taking the Laplace transform from Equation (22), we obtain:

$$\begin{aligned} \mathcal{L}(\Psi_{n,m}; s) \Psi_{n,m}(t) &= 2^{\frac{l}{2}} \sqrt{m + \frac{1}{2}} \mathcal{L}(\lambda_{\frac{2n-2}{2^l} t_f} \mathbb{P}_m \left[\frac{2^l}{t_f} (t - \frac{2n-2}{2^l} t_f) - 1 \right]; s) \\ &\quad - 2^{\frac{l}{2}} \sqrt{m + \frac{1}{2}} \mathcal{L}(\lambda_{\frac{2n}{2^l} t_f} \mathbb{P}_m \left[\frac{2^l}{t_f} (t - \frac{2n}{2^l} t_f) + 1 \right]; s) \\ &= 2^{\frac{l}{2}} \sqrt{m + \frac{1}{2}} e^{-\frac{2n-2}{2^l} t_f s} \mathcal{L}(\mathbb{P}_m \left[\frac{2^l}{t_f} t - 1 \right]; s) \end{aligned}$$

$$-2^{\frac{l}{2}} \sqrt{m + \frac{1}{2}} e^{-\frac{2n-2}{2^l} t_f s} \mathcal{L}(\mathbb{P}_m[\frac{2^l}{t_f} t + 1]; s). \quad (23)$$

By applying the definition $\mathbb{P}_m(t)$, we have:

$$\begin{aligned} \mathcal{L}(\Psi_{n,m}; s) &= 2^{\frac{l}{2}} \sqrt{m + \frac{1}{2}} e^{-\frac{2n-2}{2^l} t_f s} \mathcal{L}(2^m \sum_{k=0}^m (\frac{2^l}{t_f} t - 1)^k \binom{m}{k} \binom{\frac{m+k-1}{2}}{m}; s) \\ &= -2^{\frac{l}{2}} \sqrt{m + \frac{1}{2}} e^{-\frac{2n-2}{2^l} t_f s} \mathcal{L}(2^m \sum_{k=0}^m (\frac{2^l}{t_f} t + 1)^k \binom{m}{k} \binom{\frac{m+k-1}{2}}{m}; s) \\ &= 2^{\frac{l}{2}+m} \sqrt{m + \frac{1}{2}} e^{-\frac{2n-2}{2^l} t_f s} \sum_{k=0}^m \binom{m}{k} \binom{\frac{m+k-1}{2}}{m} \\ &\quad \times \{e^{\frac{2t_f s}{2^l}} \mathcal{L}(\frac{2^l}{t_f} - 1)^k; s) - \mathcal{L}(\frac{2^l}{t_f} + 1)^k; s)\}. \end{aligned} \quad (24)$$

Using the definition of binomial expansion, we obtain:

$$\begin{aligned} \mathcal{L}(\Psi_{n,m}; s) &= 2^{\frac{l}{2}+m} \sqrt{m + \frac{1}{2}} e^{-\frac{2n-2}{2^l} t_f s} \sum_{k=0}^m \binom{m}{k} \binom{\frac{m+k-1}{2}}{m} \\ &\quad \times \{e^{\frac{2t_f s}{2^l}} \mathcal{L}(\sum_{r=0}^k \binom{k}{r} (-1)^r (\frac{2^l}{t_f} t)^{k-r}; s) - \mathcal{L}(\sum_{r=0}^k \binom{k}{r} (\frac{2^l}{t_f} t)^{k-r}; s)\} \\ &= 2^{\frac{l}{2}+m} \sqrt{m + \frac{1}{2}} e^{-\frac{2n-2}{2^l} t_f s} \\ &\quad \times \sum_{k=0}^m \sum_{r=0}^k \frac{k!}{r!} \binom{m}{k} \binom{\frac{m+k-1}{2}}{m} (\frac{2^l}{t_f})^{k-r} (e^{\frac{2s}{2^l}} (-1)^r - 1) \frac{1}{s^{k-r+1}}. \end{aligned} \quad (25)$$

Then, the result is proved.

Theorem 3 Let $\Psi_{n,m}(t)$ be the Legendre wavelets optimization functions which is introduced in Equation (16). Then, we have:

$$\mathbb{E}_{\rho, \alpha, \omega, 0}^{\gamma} \Psi_{n,m}(t) = \begin{cases} 0, & t \in [0, \frac{2n-2}{2^l} t_f], \\ 2^{\frac{l}{2}+m} \sqrt{m + \frac{1}{2}} \sum_{k=0}^m \sum_{r=0}^k \frac{k!}{r!} \binom{m}{k} \binom{\frac{m+k-1}{2}}{m} (-1)^r t^{\alpha+k-r-2} \\ \times E_{\rho, \alpha+k-r-1}^{\gamma} (\omega(t - \frac{2n-2}{2^l} t_f)^{\rho}), & t \in [\frac{2n-2}{2^l} t_f, \frac{2n}{2^l} t_f], \\ 2^{\frac{l}{2}+m} \sqrt{m + \frac{1}{2}} \sum_{k=0}^m \sum_{r=0}^k \frac{k!}{r!} \binom{m}{k} \binom{\frac{m+k-1}{2}}{m} \times [(-1)^r t^{\alpha+k-r-2} \\ \times E_{\rho, \alpha+k-r-1}^{\gamma} (\omega(t - \frac{2n-2}{2^l} t_f)^{\rho}) - (-1)^r t^{\alpha+k-r-2} \times E_{\rho, \alpha+k-r-1}^{\gamma} (\omega(t - \frac{2n-2}{2^l} t_f)^{\rho})], & t > \frac{2n}{2^l} t_f. \end{cases}$$

Proof. Applying the definitions of Prabhakar integral and the Laplace transform, we have:

$$\begin{aligned} \mathcal{L}(\mathbb{E}_{\rho, \alpha, \omega, 0}^{\gamma} \Psi_{n,m}(t); s) &= \mathcal{L}(t^{\alpha-1} E_{\rho, \alpha}^{\gamma} (\omega t^{\rho}) * \Psi_{n,m}(t); s) \\ &= \mathcal{L}(t^{\alpha-1} E_{\rho, \alpha}^{\gamma} (\omega t^{\rho}); s) \times \mathcal{L}(\Psi_{n,m}(t); s), \end{aligned} \quad (26)$$

where $*$ is the convolution operator. Using the Theorem 2 and the Lemma 1, yields:

$$\begin{aligned} \mathcal{L}(\mathbb{E}_{\rho, \alpha, \omega, 0}^{\gamma} \Psi_{n,m}(t); s) &= 2^{\frac{l}{2}+m} \sqrt{m + \frac{1}{2}} e^{-\frac{2n-2}{2^l} t_f s} \\ &\quad \times \sum_{k=0}^m \sum_{r=0}^k \frac{k!}{r!} \binom{m}{k} \binom{\frac{m+k-1}{2}}{m} (\frac{2^l}{t_f})^{k-r} (e^{\frac{2s}{2^l}} (-1)^r - 1) \frac{1}{s^{k-r+1+\alpha(1-\omega s^{-\rho})\gamma}}. \end{aligned} \quad (27)$$

Applying both sides of Equation (27) by inverse Laplace transform yields:

$$\mathbb{E}_{\rho, \alpha, \omega, 0}^{\gamma} \Psi_{n,m}(t) = 2^{\frac{l}{2}+m} \sqrt{m + \frac{1}{2}} \sum_{k=0}^m \sum_{r=0}^k \frac{k!}{r!} \binom{m}{k} \binom{\frac{m+k-1}{2}}{m} (\frac{2^l}{t_f})^{k-r}$$

$$\begin{aligned}
& \times \mathcal{L}^{-1} \left(\frac{e^{-\frac{2n-2}{2^l} t_f s} (-1)^r}{s^{k-r+1+\alpha(1-\omega s^{-\rho})\gamma}} - \frac{e^{-\frac{2n}{2^l} t_f s}}{s^{k-r+1+\alpha(1-\omega s^{-\rho})\gamma}}; t \right) \\
& = 2^{\frac{l}{2}+m} \sqrt{m + \frac{1}{2}} \sum_{k=0}^m \sum_{r=0}^k \frac{k!}{r!} \binom{m}{k} \binom{\frac{m+k-1}{2}}{m} \left(\frac{2^l}{t_f}\right)^{k-r} \\
& \times [\lambda_{\frac{2n-2}{2^l} t_f} (-1)^r t^{\alpha+k-r-2} E_{\rho, \alpha+k-r-1}^\gamma (\omega(t - \frac{2n-2}{2^l} t_f)^\rho) \\
& - \lambda_{\frac{2n}{2^l} t_f} t^{\alpha+k-r-2} E_{\rho, \alpha+k-r-1}^\gamma (\omega(t - \frac{2n}{2^l} t_f)^\rho)]. \tag{28}
\end{aligned}$$

By applying equation (28), we consider the following three cases:

Case 1: for $t \in [0, \frac{2n-2}{2^l} t_f)$, we have $\mathbb{E}_{\rho, \alpha, \omega, 0}^\gamma \Psi_{n, m}(t) = 0$.

Case 2: for $t \in [\frac{2n-2}{2^l} t_f, \frac{2n}{2^l} t_f)$, we have:

$$\begin{aligned}
\mathbb{E}_{\rho, \alpha, \omega, 0}^\gamma \Psi_{n, m}(t) & = 2^{\frac{l}{2}+m} \sqrt{m + \frac{1}{2}} \sum_{k=0}^m \sum_{r=0}^k \frac{k!}{r!} \binom{m}{k} \binom{\frac{m+k-1}{2}}{m} (-1)^r t^{\alpha+k-r-2} \\
& \times E_{\rho, \alpha+k-r-1}^\gamma (\omega(t - \frac{2n-2}{2^l} t_f)^\rho), \tag{29}
\end{aligned}$$

Case 3: for $t > \frac{2n}{2^l} t_f$, we have:

$$\begin{aligned}
\mathbb{E}_{\rho, \alpha, \omega, 0}^\gamma \Psi_{n, m}(t) & = 2^{\frac{l}{2}+m} \sqrt{m + \frac{1}{2}} \sum_{k=0}^m \sum_{r=0}^k \frac{k!}{r!} \binom{m}{k} \binom{\frac{m+k-1}{2}}{m} \\
& \times [(-1)^r t^{\alpha+k-r-2} E_{\rho, \alpha+k-r-1}^\gamma (\omega(t - \frac{2n-2}{2^l} t_f)^\rho) - \\
& (-1)^r t^{\alpha+k-r-2} E_{\rho, \alpha+k-r-1}^\gamma (\omega(t - \frac{2n}{2^l} t_f)^\rho)]. \tag{30}
\end{aligned}$$

Then, the proof of this theorem is ended.

4 Solution of the COVID-19 model

In this Section, we study a matrix numerical method to approximate the solution of the COVID-19 model (1). For this aim, we apply Legendre wavelets optimization functions to numerically solve the COVID-19 model (1) and (2). We first approximate the Caputo derivative of the unknown function $S(t), I(t), D(t), A(t), R(t), T(t), H(t)$ and $E(t)$ applying Equation (18) as follows:

$$\begin{aligned}
{}^{CP} \mathbb{D}_{\rho, \alpha, \omega}^\gamma S(t) & \cong D_1^T \mathbb{B}(t), \\
{}^{CP} \mathbb{D}_{\rho, \alpha, \omega}^\gamma I(t) & \cong D_2^T \mathbb{B}(t), \\
{}^{CP} \mathbb{D}_{\rho, \alpha, \omega}^\gamma D(t) & \cong D_3^T \mathbb{B}(t), \\
{}^{CP} \mathbb{D}_{\rho, \alpha, \omega}^\gamma A(t) & \cong D_4^T \mathbb{B}(t), \\
{}^{CP} \mathbb{D}_{\rho, \alpha, \omega}^\gamma R(t) & \cong D_5^T \mathbb{B}(t), \\
{}^{CP} \mathbb{D}_{\rho, \alpha, \omega}^\gamma T(t) & \cong D_6^T \mathbb{B}(t), \\
{}^{CP} \mathbb{D}_{\rho, \alpha, \omega}^\gamma H(t) & \cong D_7^T \mathbb{B}(t), \\
{}^{CP} \mathbb{D}_{\rho, \alpha, \omega}^\gamma E(t) & \cong D_8^T \mathbb{B}(t), \tag{31}
\end{aligned}$$

where for $i = 1, \dots, 8$, the coefficients D_i is given by:

$$D_i^T = [d_{1,0}^i(t), \dots, d_{2^{l-1},0}^i(t), d_{1,1}^i(t), \dots, d_{2^{l-1},1}^i(t), d_{1,M-1}^i(t), \dots, d_{2^{l-1},M-1}^i(t)].$$

Then, for simpleness of sentence, we let that $S(0) = 0, I(0) = 0, D(0) = 0, A(0) = 0, R(0) = 0, T(0) = 0, H(0) = 0, E(0) = 0$. By taking the Prabhakar integral from both

sides Eq. (31), we get:

$$\begin{aligned}
 S(t) &= \mathbb{E}_{\rho, \alpha, \omega, 0}^{\gamma} {}^{CP} \mathbb{D}_{\rho, \alpha, \omega}^{\gamma} S(t), \\
 I(t) &= \mathbb{E}_{\rho, \alpha, \omega, 0}^{\gamma} {}^{CP} \mathbb{D}_{\rho, \alpha, \omega}^{\gamma} I(t), \\
 D(t) &= \mathbb{E}_{\rho, \alpha, \omega, 0}^{\gamma} {}^{CP} \mathbb{D}_{\rho, \alpha, \omega}^{\gamma} D(t), \\
 A(t) &= \mathbb{E}_{\rho, \alpha, \omega, 0}^{\gamma} {}^{CP} \mathbb{D}_{\rho, \alpha, \omega}^{\gamma} A(t), \\
 R(t) &= \mathbb{E}_{\rho, \alpha, \omega, 0}^{\gamma} {}^{CP} \mathbb{D}_{\rho, \alpha, \omega}^{\gamma} R(t), \\
 T(t) &= \mathbb{E}_{\rho, \alpha, \omega, 0}^{\gamma} {}^{CP} \mathbb{D}_{\rho, \alpha, \omega}^{\gamma} T(t), \\
 H(t) &= \mathbb{E}_{\rho, \alpha, \omega, 0}^{\gamma} {}^{CP} \mathbb{D}_{\rho, \alpha, \omega}^{\gamma} H(t), \\
 E(t) &= \mathbb{E}_{\rho, \alpha, \omega, 0}^{\gamma} {}^{CP} \mathbb{D}_{\rho, \alpha, \omega}^{\gamma} E(t),
 \end{aligned} \tag{32}$$

By applying Eq. (32), yields

$$\begin{aligned}
 S(t) &\cong D_1^T \mathbb{E}_{\rho, \alpha, \omega, 0}^{\gamma} \mathbb{B}(t), \\
 I(t) &\cong D_2^T \mathbb{E}_{\rho, \alpha, \omega, 0}^{\gamma} \mathbb{B}(t), \\
 D(t) &\cong D_3^T \mathbb{E}_{\rho, \alpha, \omega, 0}^{\gamma} \mathbb{B}(t), \\
 A(t) &\cong D_4^T \mathbb{E}_{\rho, \alpha, \omega, 0}^{\gamma} \mathbb{B}(t), \\
 R(t) &\cong D_5^T \mathbb{E}_{\rho, \alpha, \omega, 0}^{\gamma} \mathbb{B}(t), \\
 T(t) &\cong D_6^T \mathbb{E}_{\rho, \alpha, \omega, 0}^{\gamma} \mathbb{B}(t), \\
 H(t) &\cong D_7^T \mathbb{E}_{\rho, \alpha, \omega, 0}^{\gamma} \mathbb{B}(t), \\
 E(t) &\cong D_8^T \mathbb{E}_{\rho, \alpha, \omega, 0}^{\gamma} \mathbb{B}(t).
 \end{aligned} \tag{33}$$

By applying the definition of the vector function $\mathbb{B}(t)$ we have:

$$\begin{aligned}
 \mathbb{E}_{\rho, \alpha, \omega, 0}^{\gamma} \mathbb{B}(t) &= [\mathbb{E}_{\rho, \alpha, \omega, 0}^{\gamma} \psi_{1,0}(t), \dots, \mathbb{E}_{\rho, \alpha, \omega, 0}^{\gamma} \psi_{1,M-1}(t), \dots, \\
 &\quad \mathbb{E}_{\rho, \alpha, \omega, 0}^{\gamma} \psi_{2^{l-1},0}(t), \dots, \mathbb{E}_{\rho, \alpha, \omega, 0}^{\gamma} \psi_{2^{l-1},M-1}(t)]^T.
 \end{aligned}$$

Assume that

$$\mathbb{E}_{\rho, \alpha, \omega, 0}^{\gamma} \Psi_{n,m}(x) \cong \mathbb{C}_{n,m}^T \Psi(x), \quad m = 0, 1, \dots, M-1, \quad n = 1, 2, \dots, 2^{l-1},$$

in which

$$\begin{aligned}
 \mathbb{C}_{n,m} &= [c_{1,0}^{n,m}, \dots, c_{1,M-1}^{n,m}, \dots, c_{2^{l-1},0}^{n,m}, \dots, c_{2^{l-1},M-1}^{n,m}]^T, \quad c_{i,j}^{n,m} = \\
 &\quad \langle \mathbb{E}_{\rho, \alpha, \omega, 0}^{\gamma} \Psi_{n,m}(t), \Psi_{p,q}(t) \rangle.
 \end{aligned}$$

Thus,

$$\begin{aligned}
 \mathbb{E}_{\rho, \alpha, \omega, 0}^{\gamma} \Psi(t) &\cong \\
 \begin{bmatrix} c_{1,0}^{1,0} & \dots & c_{1,M-1}^{1,0} & \dots & c_{2^{l-1},0}^{1,0} & \dots & c_{2^{l-1},M-1}^{1,0} \\ \vdots & \ddots & \ddots & \ddots & \ddots & \dots & \vdots \\ c_{1,0}^{2^{l-1},M-1} & \dots & c_{1,M-1}^{2^{l-1},M-1} & \dots & c_{2^{l-1},0}^{2^{l-1},M-1} & \dots & c_{2^{l-1},M-1}^{2^{l-1},M-1} \end{bmatrix} \Psi(t) \\
 &:= \mathbb{C}_{\rho, \alpha, \omega} \Psi(t),
 \end{aligned} \tag{34}$$

where $\mathbb{C}_{\rho, \alpha, \omega} \Psi(t)$ is called the Prabhakar fractional integration matrix for the Legendre wavelets optimization functions, that these coefficients are calculated in the Theorem 3. Then we have from Equations (33) and (24) that

$$\begin{aligned}
 S(t) &\cong D_1^T \mathbb{C}_{\rho, \alpha, \omega} \Psi(t), \\
 I(t) &\cong D_2^T \mathbb{C}_{\rho, \alpha, \omega} \Psi(t), \\
 D(t) &\cong D_3^T \mathbb{C}_{\rho, \alpha, \omega} \Psi(t), \\
 A(t) &\cong D_4^T \mathbb{C}_{\rho, \alpha, \omega} \Psi(t),
 \end{aligned} \tag{35}$$

$$\begin{aligned}
R(t) &\cong D_5^T \mathbb{C}_{\rho, \alpha, \omega} \Psi(t), \\
T(t) &\cong D_6^T \mathbb{C}_{\rho, \alpha, \omega} \Psi(t), \\
H(t) &\cong D_7^T \mathbb{C}_{\rho, \alpha, \omega} \Psi(t), \\
E(t) &\cong D_8^T \mathbb{C}_{\rho, \alpha, \omega} \Psi(t).
\end{aligned}$$

By applying the definition of distributed order derivative, substituting Equation (35) into Equation (1), we have:

$$\begin{aligned}
&\mathbb{B}^T(t) D_1 \int_0^1 \omega(\alpha) d\alpha = \\
&-\Psi^T(t) \mathbb{C}_{\rho, \alpha, \omega}^T D_1 (\alpha_1 \Psi^T(t) \mathbb{C}_{\rho, \alpha, \omega}^T D_2 + \alpha_2 \Psi^T(t) \mathbb{C}_{\rho, \alpha, \omega}^T D_3 \\
&\quad + \alpha_3 \Psi^T(t) \mathbb{C}_{\rho, \alpha, \omega}^T D_4 + \alpha_4 \Psi^T(t) \mathbb{C}_{\rho, \alpha, \omega}^T D_5), \\
&\mathbb{B}^T(t) D_2 \int_0^1 \omega(\alpha) d\alpha = \\
&\Psi^T(t) \mathbb{C}_{\rho, \alpha, \omega}^T D_1 (\alpha_1 \Psi^T(t) \mathbb{C}_{\rho, \alpha, \omega}^T D_2 + \alpha_2 \Psi^T(t) \mathbb{C}_{\rho, \alpha, \omega}^T D_3 \\
&\quad + \alpha_3 \Psi^T(t) \mathbb{C}_{\rho, \alpha, \omega}^T D_4 + \alpha_4 \Psi^T(t) \mathbb{C}_{\rho, \alpha, \omega}^T D_5) - (\epsilon_1 + \zeta_1 + \lambda_1) \Psi^T(t) \mathbb{C}_{\rho, \alpha, \omega}^T D_2, \\
&\mathbb{B}^T(t) D_3 \int_0^1 \omega(\alpha) d\alpha = \epsilon_1 \Psi^T(t) \mathbb{C}_{\rho, \alpha, \omega}^T D_2 - (\eta_1 + \rho_1) \Psi^T(t) \mathbb{C}_{\rho, \alpha, \omega}^T D_3, \\
&\mathbb{B}^T(t) D_4 \int_0^1 \omega(\alpha) d\alpha = \zeta_1 \Psi^T(t) \mathbb{C}_{\rho, \alpha, \omega}^T D_2 - (\theta_1 + \mu_1 + \kappa_1) \Psi^T(t) \mathbb{C}_{\rho, \alpha, \omega}^T D_4, \quad (36) \\
&\mathbb{B}^T(t) D_5 \int_0^1 \omega(\alpha) d\alpha = \eta_1 \Psi^T(t) \mathbb{C}_{\rho, \alpha, \omega}^T D_3 + \theta_1 \Psi^T(t) \mathbb{C}_{\rho, \alpha, \omega}^T D_4 - (\nu_1 + \\
&\xi_1) \Psi^T(t) \mathbb{C}_{\rho, \alpha, \omega}^T D_5, \\
&\mathbb{B}^T(t) D_6 \int_0^1 \omega(\alpha) d\alpha = \mu_1 \Psi^T(t) \mathbb{C}_{\rho, \alpha, \omega}^T D_4 + \nu_1 \Psi^T(t) \mathbb{C}_{\rho, \alpha, \omega}^T D_5 - (\sigma_1 + \\
&\tau_1) \Psi^T(t) \mathbb{C}_{\rho, \alpha, \omega}^T D_6, \\
&\mathbb{B}^T(t) D_7 \int_0^1 \omega(\alpha) d\alpha = \lambda_1 \Psi^T(t) \mathbb{C}_{\rho, \alpha, \omega}^T D_2 + \rho_1 \Psi^T(t) \mathbb{C}_{\rho, \alpha, \omega}^T D_3 \\
&\quad + \kappa_1 \Psi^T(t) \mathbb{C}_{\rho, \alpha, \omega}^T D_4 + \xi_1 \Psi^T(t) \mathbb{C}_{\rho, \alpha, \omega}^T D_5 + \sigma_1 \Psi^T(t) \mathbb{C}_{\rho, \alpha, \omega}^T D_6, \\
&\mathbb{B}^T(t) D_8 \int_0^1 \omega(\alpha) d\alpha = \tau_1 \Psi^T(t) \mathbb{C}_{\rho, \alpha, \omega}^T D_6.
\end{aligned}$$

By using the Gauss–Legendre numerical integration which is given in [37]. First, the integral in Equation (36), is computed, then, we collocate at Newton–cotes nodes t_i defined by:

$$t_i = \frac{2j-1}{2^l M}, j = 1, 2, 3, \dots, 2^{l-1} M, \quad (37)$$

we obtain

$$\begin{aligned}
&\mathbb{B}^T(t_i) D_1 \sum_{j=1}^n \left(\frac{1}{2} \varpi_j \omega \left(\frac{1}{2} - \frac{1}{2} \vartheta_j \right) \right) = -\Psi^T(t_i) \mathbb{C}_{\rho, \alpha, \omega}^T D_1 (\alpha_1 \Psi^T(t_i) \mathbb{C}_{\rho, \alpha, \omega}^T D_2 \\
&\quad + \alpha_2 \Psi^T(t_i) \mathbb{C}_{\rho, \alpha, \omega}^T D_3 + \alpha_3 \Psi^T(t_i) \mathbb{C}_{\rho, \alpha, \omega}^T D_4 + \alpha_4 \Psi^T(t_i) \mathbb{C}_{\rho, \alpha, \omega}^T D_5), \\
&\mathbb{B}^T(t_i) D_2 \sum_{j=1}^n \left(\frac{1}{2} \varpi_j \omega \left(\frac{1}{2} - \frac{1}{2} \vartheta_j \right) \right) = \Psi^T(t_i) \mathbb{C}_{\rho, \alpha, \omega}^T D_1 (\alpha_1 \Psi^T(t_i) \mathbb{C}_{\rho, \alpha, \omega}^T D_2 + \\
&\alpha_2 \Psi^T(t_i) \mathbb{C}_{\rho, \alpha, \omega}^T D_3 \\
&\quad + \alpha_3 \Psi^T(t_i) \mathbb{C}_{\rho, \alpha, \omega}^T D_4 + \alpha_4 \Psi^T(t_i) \mathbb{C}_{\rho, \alpha, \omega}^T D_5) - (\epsilon_1 + \zeta_1 + \lambda_1) \Psi^T(t_i) \mathbb{C}_{\rho, \alpha, \omega}^T D_2, \\
&\mathbb{B}^T(t_i) D_3 \sum_{j=1}^n \left(\frac{1}{2} \varpi_j \omega \left(\frac{1}{2} - \frac{1}{2} \vartheta_j \right) \right) = \\
&\epsilon_1 \Psi^T(t_i) \mathbb{C}_{\rho, \alpha, \omega}^T D_2 - (\eta_1 + \rho_1) \Psi^T(t_i) \mathbb{C}_{\rho, \alpha, \omega}^T D_3, \\
&\mathbb{B}^T(t_i) D_4 \sum_{j=1}^n \left(\frac{1}{2} \varpi_j \omega \left(\frac{1}{2} - \frac{1}{2} \vartheta_j \right) \right) = \zeta_1 \Psi^T(t_i) \mathbb{C}_{\rho, \alpha, \omega}^T D_2 - (\theta_1 + \mu_1 + \\
&\kappa_1) \Psi^T(t_i) \mathbb{C}_{\rho, \alpha, \omega}^T D_4, \quad (38) \\
&\mathbb{B}^T(t_i) D_5 \sum_{j=1}^n \left(\frac{1}{2} \varpi_j \omega \left(\frac{1}{2} - \frac{1}{2} \vartheta_j \right) \right) = \\
&\eta_1 \Psi^T(t_i) \mathbb{C}_{\rho, \alpha, \omega}^T D_3 + \theta_1 \Psi^T(t_i) \mathbb{C}_{\rho, \alpha, \omega}^T D_4 - (\nu_1 + \xi_1) \Psi^T(t_i) \mathbb{C}_{\rho, \alpha, \omega}^T D_5, \\
&\mathbb{B}^T(t_i) D_6 \sum_{j=1}^n \left(\frac{1}{2} \varpi_j \omega \left(\frac{1}{2} - \frac{1}{2} \vartheta_j \right) \right) = \\
&\mu_1 \Psi^T(t_i) \mathbb{C}_{\rho, \alpha, \omega}^T D_4 + \nu_1 \Psi^T(t_i) \mathbb{C}_{\rho, \alpha, \omega}^T D_5 - (\sigma_1 + \tau_1) \Psi^T(t_i) \mathbb{C}_{\rho, \alpha, \omega}^T D_6, \\
&\mathbb{B}^T(t_i) D_7 \sum_{j=1}^n \left(\frac{1}{2} \varpi_j \omega \left(\frac{1}{2} - \frac{1}{2} \vartheta_j \right) \right) = \lambda_1 \Psi^T(t) \mathbb{C}_{\rho, \alpha, \omega}^T D_2 + \rho_1 \Psi^T(t) \mathbb{C}_{\rho, \alpha, \omega}^T D_3 +
\end{aligned}$$

$$\begin{aligned} & \kappa_1 \Psi^T(t) \mathbb{C}_{\rho, \alpha, \omega}^T D_4 \\ & + \xi_1 \Psi^T(t_i) \mathbb{C}_{\rho, \alpha, \omega}^T D_5 + \sigma_1 \Psi^T(t_i) \mathbb{C}_{\rho, \alpha, \omega}^T D_6, \\ & \mathbb{B}^T(t_i) D_8 \sum_{j=1}^n \left(\frac{1}{2} \varpi_j \omega \left(\frac{1}{2} - \frac{1}{2} \vartheta_j \right) \right) = \tau_1 \Psi^T(t_i) \mathbb{C}_{\rho, \alpha, \omega}^T D_6, \end{aligned}$$

in which ϖ_j and ϑ_j are weights of Gauss-Bézier-Legendre and nodes of Gauss-Bézier-Legendre, respectively, that these weights of Gauss-Bézier-Legendre and nodes of Gauss-Bézier-Legendre are given in [37]. By applying the Newton's iterative method, we can be calculated the unknown parameters D_i in Equation (37). The initial guess for solving Equation (37) using the Newton's iterative method can be calculated similarly by the method studied in [38]. To select the initial guesses for solving Equation (37) using the Newton's iterative method, in the first stage, we put $l = 1$ and $M = 1$, then we solve Equation (37) applying the Newton's iterative method. In this stage, we calculate an approximation solution to our system. In the next stage, we put $l = 2$ and increase the value of M , considering the initial guess in the first stage, we obtain the approximate solution in this stage. We follow this approach until the desired results are achieved. By determining the unknown parameters D_i in Equation (37), the approximate solutions of $S(t), I(t), D(t), A(t), R(t), T(t), H(t)$ and $E(t)$ can be obtained.

5 Study and check error analysis

In this section, we present the convergence and error analysis for the proposed method. Here we define the Sobolov space of order q that q is a integer as follows:

$$H^q(a, b) = \{f \in L^2(a, b) | f^{(j)} \in L^2(a, b), 1 \leq j \leq q\}, \quad (39)$$

in which the derivative $f^{(j)} \in L^2(a, b)$ is in the sense of distribution [37].

Lemma 4 Suppose that $g \in H^q(0, 1)$, $q \geq 1$ and $I_n = [\frac{n-1}{2^{l-1}}, \frac{n}{2^{l-1}}]$. Also, let $g = \sum_{n=1}^{2^{l-1}} g_n$, that $g_n \in H^q(I_n)$. If $\mathcal{Y}_n = \text{span}\{\psi_{n,0}(x), \dots, \psi_{n,M-1}(x)\}$ and $B_n^T \psi_n(x) \in \mathcal{Y}_n$ be the best approximation of f_n , that $B_n = [b_{n,0}, \dots, b_{n,M-1}]^T$ and $\psi_n(x) = [\psi_{n,0}(x), \dots, \psi_{n,M-1}(x)]^T$. Then, we have

$$\|g - B^T \psi\|_{L^2(0,1)} \leq d(M2^{l-1})^{-q} \|g^{(q)}\|_{L^2(0,1)}, \quad (40)$$

where $B = [B_1, \dots, B_{2^{l-1}}]^T$ and d depends on q .

Proof. Let $g_n^M(x) = \sum_{n=1}^M g_n(x)$. Since $g_n^M(x)$ is the polynomial of best approximation of $g_n \in L^2$ [37]. Thus from equation (5.4.11) in Ref. [37] displayed that $q \leq M + 1$.

Lemma 5 Suppose the assumptions of the Lemma 4, hold. Then, we for $q \geq 4$ have

$$\|g' - (B^T \psi)'\|_{L^\infty(0,1)} \leq d(M2^{l-1})^{4-q} \|g^{(q)}\|_{L^2(0,1)}. \quad (41)$$

Proof. Consult [39].

Lemma 6 Suppose the assumptions of the Lemma 4, hold. Then, we for $q \geq 4$ and $0 < \alpha < 1$ have

$$\|{}_0^{CP} D_{\rho, \alpha, \omega}^\gamma (g - B^T \psi)\|_{L^\infty(0,1)} \leq d_{\gamma, \rho, \alpha, \omega} (2^{l-1})^{4+\alpha-q} M^{4-q} \|g^{(q)}\|_{L^2(0,1)}. \quad (42)$$

Proof. Using Eq. (9) and by triangular and Hölder inequalities, we obtain

$$\begin{aligned} & |{}_0^{CP} D_{\rho, \alpha, \omega}^\gamma (g - B^T \psi)(x)| \leq \sum_{n=1}^{2^{l-1}} \int_{I_n} (\sum_{i=0}^\infty P_i(x-s)^{\rho i - \alpha}) |g_n' - (g_n^M)'| ds \\ & \leq \sum_{n=1}^{2^{l-1}} \|g_n' - (g_n^M)'\|_{L^\infty(I_n)} \int_{I_n} \sum_{i=0}^\infty P_i(x-s)^{\rho i - \alpha} ds, \end{aligned}$$

in which $P_i = \frac{\Gamma(-\gamma+i)\omega^i}{\Gamma(-\gamma)\Gamma(\rho i + 1 - \alpha)i!}$. Due to the definition of the Prabhakar function the

summations inside the above integrals are convergent. Consequently, by calculating the integrals and recalling that the length of each subinterval I_n is $2^{1-l} \leq 1$, we get

$$\left| {}_0^{CP}D_{\rho,\alpha,\omega}^{\gamma}(g - B^T\psi)(x) \right| \leq \sum_{n=1}^{2^{l-1}} \|g_n' - (g_n^M)'\|_{L^\infty(I_n)} (2^{1-l})^{1-\alpha} \sum_{i=0}^{\infty} \frac{P_i}{\rho i - \alpha + 1}.$$

With a simple calculation, we have $\sum_{i=0}^{\infty} \frac{P_i}{\rho i - \alpha + 1} = E_{\rho,2-\alpha}^{-\gamma}(\omega)$. It follows from Eq. (6) that $\sum_{i=0}^{\infty} \frac{P_i}{\rho i - \alpha + 1} = E_{\rho,2-\alpha}^{-\gamma}(\omega)$. Then, we from Lemma 5 conclude that

$$\begin{aligned} \left| {}_0^{CP}D_{\rho,\alpha,\omega}^{\gamma}(g - B^T\psi)(x) \right| &\leq (2^{1-l})^{1-\alpha} E_{\rho,2-\alpha}^{-\gamma}(\omega) \sum_{n=1}^{2^{l-1}} \|g_n' - (g_n^M)'\|_{L^\infty(I_n)} \\ &\leq (2^{l-1})^\alpha E_{\rho,2-\alpha}^{-\gamma}(\omega) \|g' - (B^T\psi)'\|_{L^\infty(0,1)} \\ &\leq o_{\gamma,\rho,\alpha,\omega}(2^{l-1})^{4+\alpha-q} M^{4-q} \|g^{(q)}\|_{L^2(0,1)}. \end{aligned}$$

The above equation shows that the proof is complete.

Lemma 7 Let $g \in H^q(0,1)$ such that $q \geq 4$, $g = \sum_{n=1}^{2^{l-1}} g_n$ and $U_n^T \psi_n(x)$ be the best approximation to ${}_0^{CP}D_{\rho,\alpha,\omega}^{\gamma} g_n$ from Y_n . Then for $\alpha \in (0,1)$ we get the following inequality:

$$\|g - U^T C_{\gamma,\rho,\alpha,\omega} \psi\|_{L^2(0,1)} \leq o_{\gamma,\rho,\alpha,\omega}(2^{l-1})^{5-q} M^{4-q} \|g^{(q)}\|_{L^2(0,1)}. \quad (43)$$

Proof. Let $g(x) = \mathbf{E}_{\rho,\alpha,\omega,0}^{\gamma} {}_0^{CP} D_{\rho,\alpha,\omega}^{\gamma} g(x)$, than due to Eq. (34), we have $U^T \mathbf{C}_{\rho,\alpha,\omega} \Psi(x) = \mathbf{E}_{\rho,\alpha,\omega,0}^{\gamma} U^T \psi(x)$. Then,

$$|g(x) - U^T C_{\gamma,\rho,\alpha,\omega} \psi(x)| = |\mathbf{E}_{\rho,\alpha,\omega,0}^{\gamma} ({}_0^{CP} D_{\rho,\alpha,\omega}^{\gamma} g(x) - U^T \psi(x))|$$

applying the equation (7) and by triangular and Hölder inequalities, we get

$$\begin{aligned} |g(x) - U^T C_{\gamma,\rho,\alpha,\omega} \psi(x)| &\leq \\ \sum_{n=1}^{2^{l-1}} \int_{I_n} (\sum_{i=0}^{\infty} Q_i (x-s)^{\rho i + \alpha - 1}) |{}_0^{CP} D_{\rho,\alpha,\omega}^{\gamma} (g_n - g_n^M)| ds &\leq \\ \sum_{n=1}^{2^{l-1}} \|{}_0^{CP} D_{\rho,\alpha,\omega}^{\gamma} (g_n - g_n^M)\|_{L^\infty(I_n)} \int_{I_n} \sum_{i=0}^{\infty} Q_i (x-s)^{\rho i + \alpha - 1} ds, \end{aligned}$$

in which $Q_i = \frac{\Gamma(\gamma+i)\omega^i}{\Gamma(\gamma)\Gamma(\rho i + \alpha)i!}$. With a similar process in the proof of Lemma 6, we get

$$\begin{aligned} |g(x) - U^T C_{\gamma,\rho,\alpha,\omega} \psi(x)| &\leq \\ \sum_{n=1}^{2^{l-1}} \|{}_0^{CP} D_{\rho,\alpha,\omega}^{\gamma} (g_n - g_n^M)\|_{L^\infty(I_n)} (2^{1-l})^\alpha \sum_{i=0}^{\infty} \frac{Q_i}{\rho i + \alpha} &\leq \\ \text{Because } \sum_{i=0}^{\infty} \frac{P_i}{\rho i + \alpha} = E_{\rho,\alpha+1}^{\gamma}(\omega). \text{ Then, we from Lemma 6 have} & \\ |g(x) - U^T C_{\gamma,\rho,\alpha,\omega} \psi(x)| &\leq (2^{1-l})^\alpha E_{\rho,\alpha+1}^{\gamma}(\omega) \sum_{n=1}^{2^{l-1}} \|{}_0^{CP} D_{\rho,\alpha,\omega}^{\gamma} (g_n - g_n^M)\|_{L^\infty(I_n)} \\ &\leq (2^{l-1})^{1-\alpha} E_{\rho,\alpha+1}^{\gamma}(\omega) \|{}_0^{CP} D_{\rho,\alpha,\omega}^{\gamma} (g - B^T \psi)\|_{L^\infty(0,1)} \\ &\leq o_{\gamma,\rho,\alpha,\omega}(2^{l-1})^{5-q} M^{4-q} \|g^{(q)}\|_{L^2(0,1)}. \end{aligned}$$

It follows that

$$\begin{aligned} \|g - U^T \mathbf{C}_{\rho,\alpha,\omega} \psi\|_{L^2(0,1)}^2 &= \int_0^1 |g(x) - U^T \mathbf{C}_{\rho,\alpha,\omega} \psi(x)|^2 dx \\ &\leq o_{\gamma,\rho,\alpha,\omega}^2 (2^{l-1})^{10-2q} M^{8-2q} \|g^{(q)}\|_{L^2(0,1)}^2, \end{aligned} \quad (44)$$

that completes the proof.

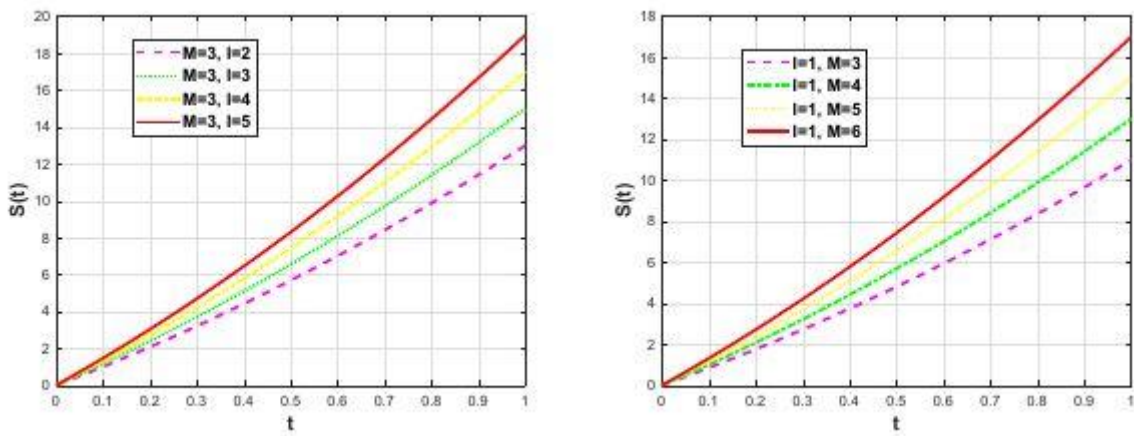


Fig. 1 Numerical experiments of susceptible class for $\alpha = 0.5$, $\rho = \omega = 1$ and various values of l and M .

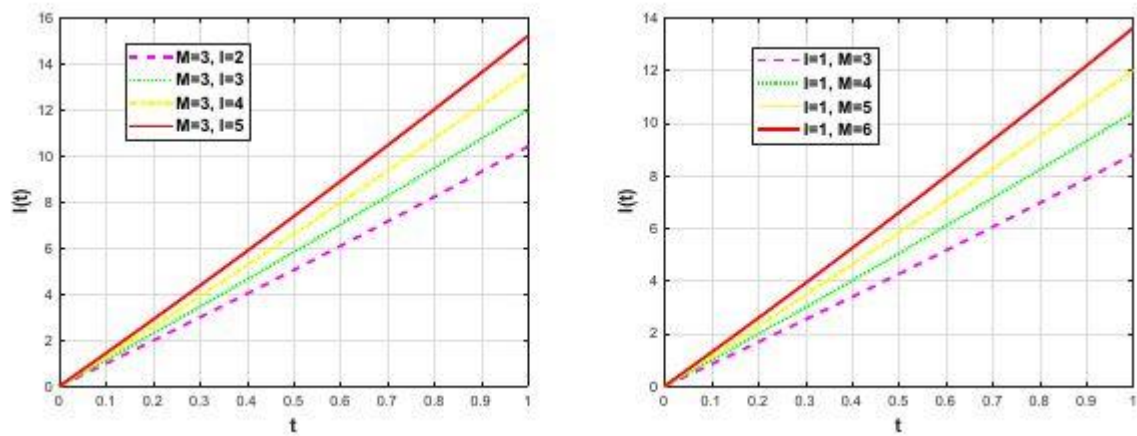


Fig. 2 Numerical experiments of infected asymptomatic infected undetected class for $\alpha = 0.5$, $\rho = \omega = 1$ and various values of l and M .

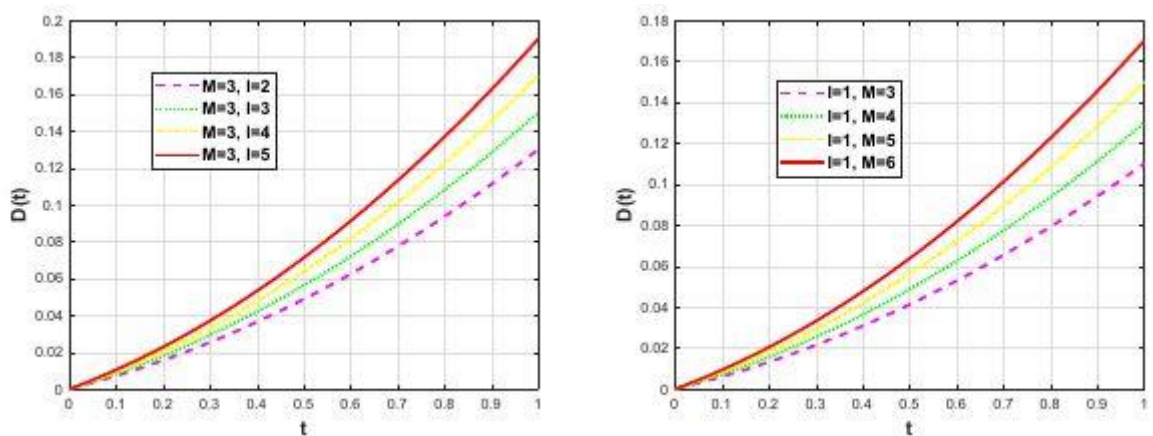


Fig. 3 Numerical experiments of asymptomatic infected class for $\alpha = 0.5$, $\rho = \omega = 1$ and various values of l and M .

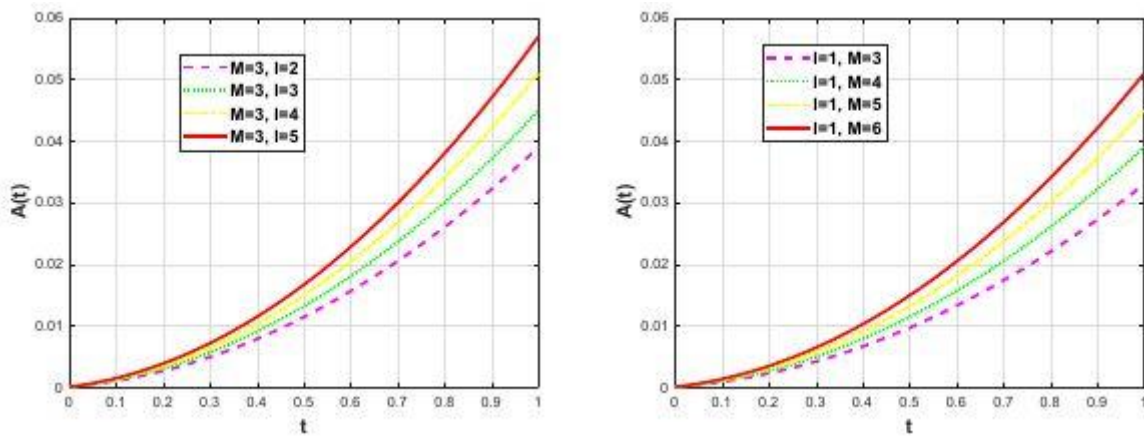


Fig. 4 Numerical experiments of healed class for $\alpha = 0.5$, $\rho = \omega = 1$ and various values of l and M .

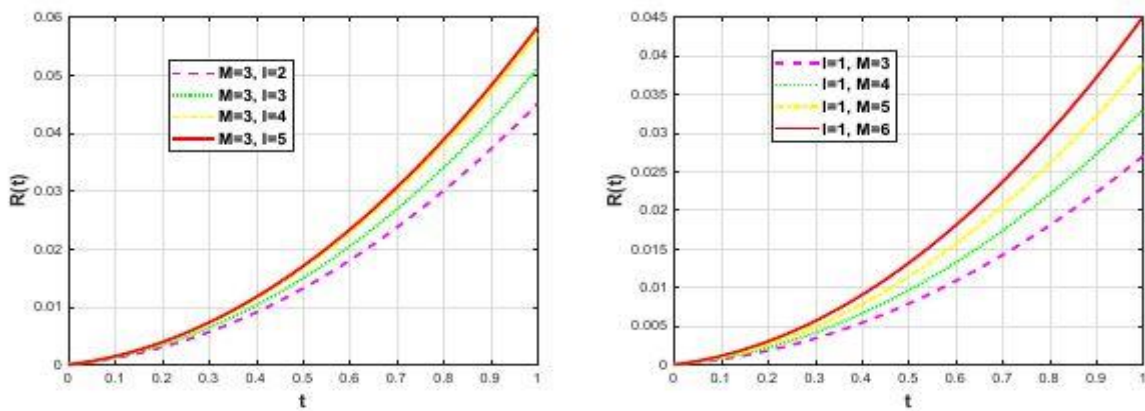


Fig. 5 Numerical experiments of ailing symptomatic infected class for $\alpha = 0.5$, $\rho = \omega = 1$ and various values of l and M .

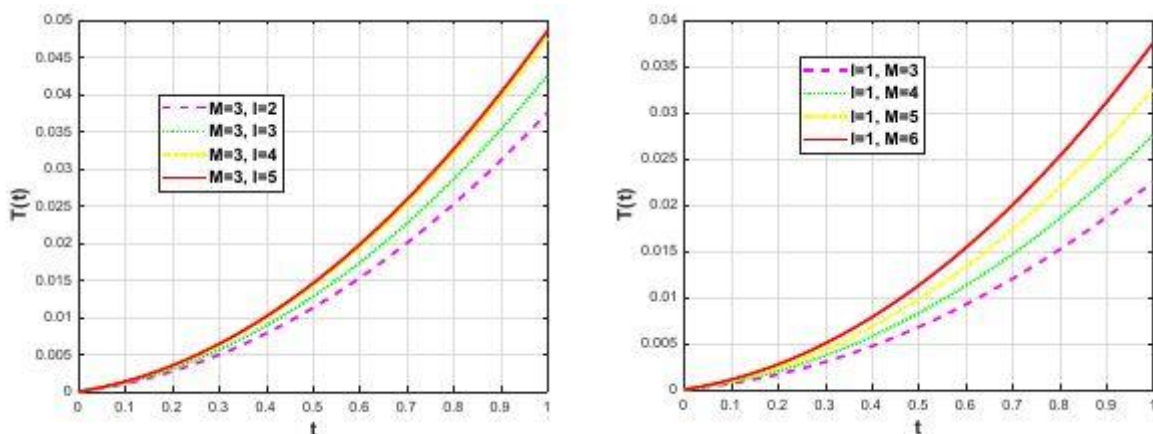


Fig. 6 Numerical experiments of recognized symptomatic infected class for $\alpha = 0.5$, $\rho = \omega = 1$ and various values of l and M .

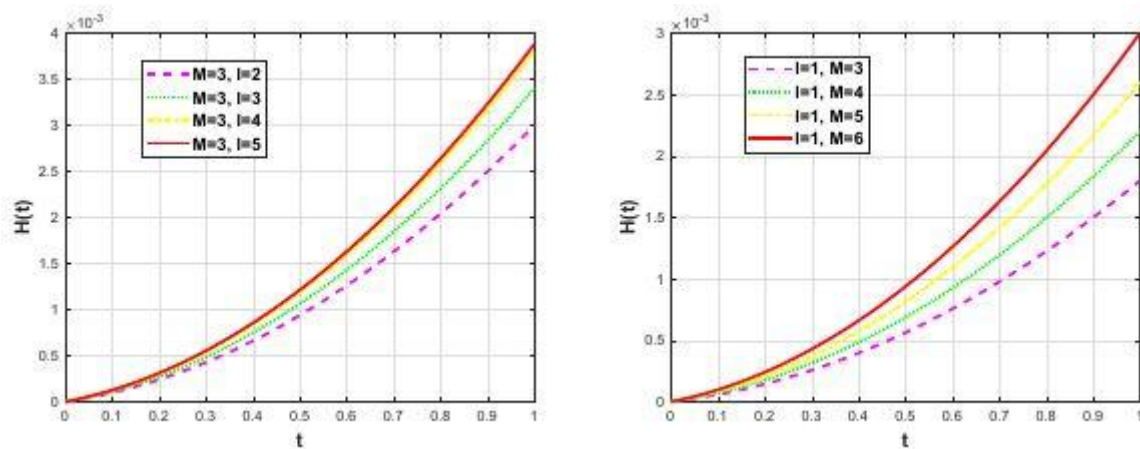


Fig. 7 Numerical experiments of acutely symptomatic infected detected class for $\alpha = 0.5$, $\rho = \omega = 1$ and various values of l and M .

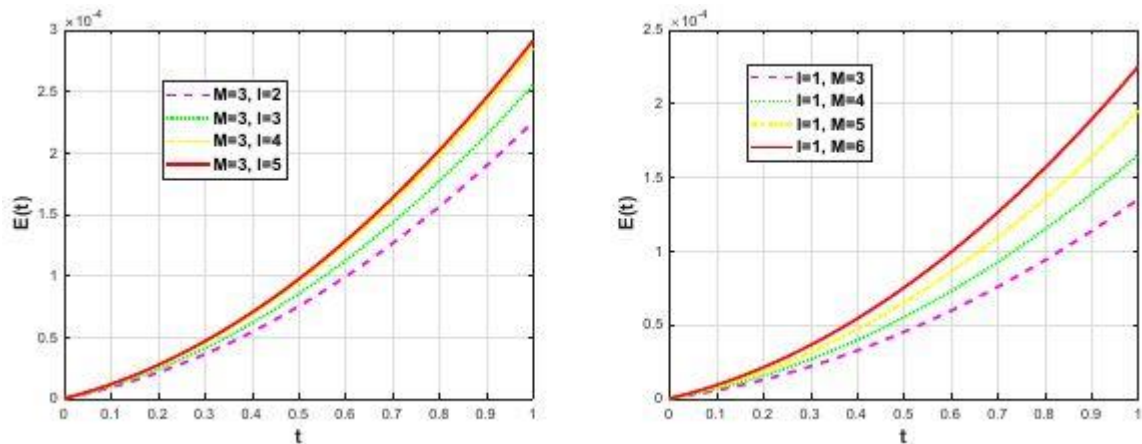


Fig. 8 Numerical experiments of death class for $\alpha = 0.5$, $\rho = \omega = 1$ and various values of l and M .

6 Numerical experiments

Measurement-induced COVID-19 conductions demonstrate an interesting and attracting novel class of phase conduction which appear light on the resilience of the present type of viruses against a known one. They were initially discovered for systems at integrable models and ordinary differential equations dynamics. To show the practicability and the efficiency of the proposed approximation method based on upon Legendre wavelets optimization approach, we demonstrate test examples and find their approximation solution via the method discussed in the previous section. We apply the proposed approximation method to numerically solve the system (1) to investigate the accuracy and capability of the proposed method. Moreover, for all cases, we put $t_f = 1$. In all computations, we use here all the computations done in Matlab (R2020b) software for the problems implemented in numerical experiments and all obtained numerical results are computed with ten considerable digits. Taking $t_i = \frac{2^{j-1}}{2^l M}, j = 1, 2, 3, \dots, 2^{l-1} M$, we have solved this given model in Equation (1) with various values of l and M . The numerical results for $\alpha = 0.5$ and various values of l and M are shown in Figs. 1-7 and 8. To show the behavior of this virus model with contacting to infected or

asymptotically infected, we demonstrated the graph of the approximate solutions of $S(t), I(t), D(t), A(t), R(t), T(t), H(t)$ and $E(t)$ for $\alpha = 0.5$ and various values of l and M . In Figs. 1-7 and 8, the approximate solutions of $S(t), I(t), D(t), A(t), R(t), T(t), H(t)$ and $E(t)$ obtained by the proposed method plotted by $l = 2,3,4,5$ and $M = 3$ (left) and $l = 1, M = 3,4,5,6$ (right) are shown. Fig. 1 display the approximate solutions of the class of susceptible for $\alpha = 0.5$ and various values of l and M . Fig. 2 display the approximate solutions of the class of infected asymptomatic, infected undetected and detected for $\alpha = 0.5$ and various values of l and M . Fig. 3 display the approximate solutions of the class of asymptomatic infected for $\alpha = 0.5$ and various values of l and M . Fig. 4 display the approximate solutions of the ailing symptomatic infected, undetected for $\alpha = 0.5$ and various values of l and M . Fig. 5 display the approximate solutions of the symptomatic infected and detected for $\alpha = 0.5$ and various values of l and M . Fig. 6 display the approximate solutions of the class of acutely symptomatic infected detected for $\alpha = 0.5$ and various values of l and M . Fig. 7 display the approximate solutions of the healed class for $\alpha = 0.5$ and various values of l and M . Fig. 8 display the approximate solutions of the death class for $\alpha = 0.5$ and various values of l and M .

7 Conclusion

In this paper, a computational approach based on the upon Legendre wavelets optimization approximations is proposed for acquiring an approximate solution of distributed order time fractional Coronavirus-19 disease model where the time-fractional operator are given in the Caputo-Prabhakar sense. To acquire the numerical solution of distributed order time fractional Coronavirus-19 disease model, we made an exact formula for the Prabhakar fractional integral operator by using the Legendre wavelets optimization functions. Then by using this exact formula and the properties of Legendre wavelets optimization functions, we reduce the presented model into a system of algebraic equations, that these system of algebraic equations have been solved by using the Newton's iterative method. In addition to, in this study, the Legendre wavelets optimization functions and their significant properties are presented. Error analysis of the approximation method is examined. The numerical example is plotted to show the practical efficiency and accuracy of the proposed numerical method. The high applicability of the given results in this paper show the practical applicability and high accuracy the considered method. Also, The solutions are approximated by applying the presented method with $\alpha \in (0,1]$, $t \in [0,1]$ and different values of parameters as M, l and from the results of figures and tables, we see that the growth of convergence increases with increasing value M . In addition to, the results of figures and tables show that the proposed numerical algorithm is simple and effective allowing a more assertive analysis of the COVID-19 model.

References

1. Giordano, G., Blanchini, F., Bruno, R., Colaneri, P., Di Filippo, A., Di Matteo, A., & Colaneri, M. (2020). Modelling the COVID-19 epidemic and implementation of population-wide interventions in Italy. *Nature medicine*, 26(6), 855-860.
2. Aminikhah, H., Refahi Sheikhani, A., & Rezazadeh, H. (2013). Stability analysis of distributed order fractional Chen system. *The Scientific World Journal*, 2013.
3. Bagley, R. L., & Torvik, P. J. (1983). A theoretical basis for the application of fractional calculus to

- viscoelasticity. *Journal of Rheology*, 27(3), 201-210.
4. Podlubny, I., Chechkin, A., Skovranek, T., Chen, Y., & Jara, B. M. V. (2009). Matrix approach to discrete fractional calculus II: Partial fractional differential equations. *Journal of Computational Physics*, 228(8), 3137-3153.
 5. Mahboob Dana, Z., Najafi, H. S., & Refahi Sheikhani, A. H. (2020). An efficient numerical method for solving Benjamin–Bona–Mahony–Burgers equation using difference scheme. *Journal of difference equations and applications*, 26(4), 574-585.
 6. Oldham, K., & Spanier, J. (1974). The fractional calculus theory and applications of differentiation and integration to arbitrary order. Elsevier.
 7. Caputo, M. (1995). Mean fractional-order-derivatives differential equations and filters. *Annali dell'Università di Ferrara*, 41(1), 73-84.
 8. Atanackovic, T. M. (2002). A generalized model for the uniaxial isothermal deformation of a viscoelastic body. *Acta Mechanica*, 159, 77-86.
 9. Fei, M., & Huang, C. (2020). Galerkin–Legendre spectral method for the distributed-order time fractional fourth-order partial differential equation. *International Journal of Computer Mathematics*, 97(6), 1183-1196.
 10. Zaky, M. A., Doha, E. H., & Tenreiro Machado, J. A. (2018). A spectral numerical method for solving distributed-order fractional initial value problems. *Journal of Computational and Nonlinear Dynamics*, 13(10), 101007.
 11. Zhang, H., Liu, F., Jiang, X., Zeng, F., & Turner, I. (2018). A Crank–Nicolson ADI Galerkin–Legendre spectral method for the two-dimensional Riesz space distributed-order advection–diffusion equation. *Computers & Mathematics with Applications*, 76(10), 2460-2476.
 12. Xu, Y., Zhang, Y., & Zhao, J. (2019). Error analysis of the Legendre–Gauss collocation methods for the nonlinear distributed-order fractional differential equation. *Applied Numerical Mathematics*, 142, 122-138.
 13. Dehghan, M., & Abbaszadeh, M. (2018). A Legendre spectral element method (SEM) based on the modified bases for solving neutral delay distributed-order fractional damped diffusion-wave equation. *Mathematical Methods in the Applied Sciences*, 41(9), 3476-3494.
 14. Guo, S., Mei, L., Zhang, Z., & Jiang, Y. (2018). Finite difference/spectral-Galerkin method for a two-dimensional distributed-order time–space fractional reaction–diffusion equation. *Applied Mathematics Letters*, 85, 157-163.
 15. Morgado, M. L., Rebelo, M., Ferras, L. L., & Ford, N. J. (2017). Numerical solution for diffusion equations with distributed order in time using a Chebyshev collocation method. *Applied numerical mathematics*, 114, 108-123.
 16. Mashayekhi, S., & Razzaghi, M. (2016). Numerical solution of distributed order fractional differential equations by hybrid functions. *Journal of computational physics*, 315, 169-181.
 17. Gorenflo, R., Luchko, Y., & Stojanović, M. (2013). Fundamental solution of a distributed order time-fractional diffusion-wave equation as probability density. *Fractional Calculus and Applied Analysis*, 16, 297-316.
 18. Li, X. Y., & Wu, B. Y. (2016). A numerical method for solving distributed order diffusion equations. *Applied mathematics letters*, 53, 92-99.
 19. Aminikhah, H., Sheikhani, A. H. R., & Rezazadeh, H. (2018). Approximate analytical solutions of distributed order fractional Riccati differential equation. *Ain shams engineering journal*, 9(4), 581-588.
 20. Mashoof, M., Refahi Sheikhani, A. H., & Saberi Najafi, H. (2018). Stability analysis of distributed-order Hilfer–Prabhakar systems based on Inertia theory. *Mathematical notes*, 104, 74-85.
 21. Mashoof, M., Sheikhani, A. R., & NAJA, H. S. (2018). Stability analysis of distributed order Hilfer–Prabhakar differential equations. *Hacettepe journal of mathematics and statistics*, 47(2), 299-315.
 22. Aminikhah, H., Sheikhani, A. H. R., Houlari, T., & Rezazadeh, H. (2017). Numerical solution of the distributed-order fractional Bagley–Torvik equation. *IEEE/CAA journal of automatica Sinica*, 6(3), 760-765.
 23. Ye, H., Liu, F., & Anh, V. (2015). Compact difference scheme for distributed-order time-fractional diffusion-wave equation on bounded domains. *Journal of Computational Physics*, 298, 652-660.
 24. Mashoof, M., & Sheikhani, A. R. (2017). Simulating the solution of the distributed order fractional differential equations by block-pulse wavelets. *UPB Sci. Bull., Ser. A: Appl. Math. Phys*, 79, 193-206.
 25. Yuttanan, B., & Razzaghi, M. (2019). Legendre wavelets approach for numerical solutions of distributed order fractional differential equations. *Applied Mathematical Modelling*, 70, 350-364.
 26. Ford, N. J., & Morgado, M. L. (2012). Distributed order equations as boundary value problems. *Computers & Mathematics with Applications*, 64(10), 2973-2981.
 27. Luchko, Y. (2009). Boundary value problems for the generalized time-fractional diffusion equation of distributed order. *Fract. Calc. Appl. Anal.*, 12(4), 409-422.
 28. Bhrawy, A. H., & Zaky, M. A. (2017). Numerical simulation of multi-dimensional distributed-order

- generalized Schrödinger equations. *Nonlinear Dynamics*, 89, 1415-1432.
29. Kharazmi, E., & Zayernouri, M. (2018). Fractional pseudo-spectral methods for distributed-order fractional PDEs. *International Journal of Computer Mathematics*, 95(6-7), 1340-1361.
30. Diethelm, K., & Ford, N. J. (2002). Analysis of fractional differential equations. *Journal of Mathematical Analysis and Applications*, 265(2), 229-248.
31. Mashoof, M., & Sheikhani, A. R. (2016). Numerical solution of fractional control system by Haar-wavelet operational matrix method. *Int. J. Industrial Mathematics*, 8, 289-298.
32. Aminikhah, H., Refahi Sheikhani, A. H., & Rezazadeh, H. (2016). Sub-equation method for the fractional regularized long-wave equations with conformable fractional derivatives. *Scientia Iranica*, 23(3), 1048-1054.
33. Aminikhah, H., Refahi Sheikhani, A. H., & Rezazadeh, H. (2014). Exact and numerical solutions of linear and non-linear systems of fractional partial differential equations. *Journal of Mathematical Modeling*, 2(1), 22-40.
34. Garra, R., & Garrappa, R. (2018). The Prabhakar or three parameter Mittag-Leffler function: Theory and application. *Communications in Nonlinear Science and Numerical Simulation*, 56, 314-329.
35. Duong, P. L. T., Kwok, E., & Lee, M. (2016). Deterministic analysis of distributed order systems using operational matrix. *Applied Mathematical Modelling*, 40(3), 1929-1940.
36. Razzaghi, M., & Yousefi, S. (2001). The Legendre wavelets operational matrix of integration. *International journal of systems science*, 32(4), 495-502.
37. Canuto, C., Hussaini, M. Y., Quarteroni, A., & Zang, T. A. (2007). *Spectral methods: fundamentals in single domains*. Springer Science & Business Media.
38. Mashayekhi, S., Ordokhani, Y., & Razzaghi, M. (2013). A hybrid functions approach for the Duffing equation. *Physica Scripta*, 88(2), 025002.
39. Maleki, M., Hashim, I., Abbasbandy, S., & Alsaedi, A. (2015). Direct solution of a type of constrained fractional variational problems via an adaptive pseudospectral method. *Journal of Computational and Applied Mathematics*, 283, 41-57.